The Effect of SiO_2 Porosity on Activity Profiles and Comonomer Incorporation in Slurry Ethylene/Butene-1 Polymerization by (SiO_2/$MgCl_2$/TEOS/$TiCl_4$) Catalyst System

Mohammad Vakili,[1,2] Hassan Arabi,[1] Hamid Salehi Mobarakeh[1]

[1]*Iran Polymer and Petrochemical Institute, Tehran, Iran*
[2]*Natural Petrochemical Company Research and Technology (NPC-RT), Tehran, Iran*

Received 3 August 2010; accepted 7 October 2010
DOI 10.1002/app.33560
Published online 13 December 2011 in Wiley Online Library (wileyonlinelibrary.com).

ABSTRACT: To investigate the influence of support porosity parameters e.g., average pore volume (APV), pore diameter (PD), and pore surface area distribution (PSAD) on activity-profile of catalyst and comonomer incorporation, a series of silica-supports with different porosity were prepared through sol–gel method and used to synthesize corresponding (SiO_2/$MgCl_2$/TEOS/$TiCl_4$) catalysts. Polymerization of ethylene/butene-1 showed that increasing of APV from 0.75 to 2.2 cm^3 g^{-1}_{SiO2} increase initial activity from 120 to 400 (g_{poly}/g_{cat}.bar.hr) followed by appearance of secondary peaks in activity-profile which could be attributed to the variation of PSAD. It is found that the effect of support in polymerization is a complicated issue which depends not only on the porosity parameters also on the comonomer concentration. The catalyst with PD of 300 Å gives higher comonomer incorporation and polymers with 15–20% lower crystallinity in contrast to catalyst with PD of 100 Å. Porosity effect was quantitatively studied by modifying of conventional Z-N catalyst polymerization mechanism through introducing fragmentation term to achieve a new tool in designing and developing of polyolefin catalysts.
 J Appl Polym Sci 124: 5145–5153, 2012

Key words: Ziegler-Natta; polymerization catalyst; porosity; activity profile; fragmentation; comonomer incorporation

INTRODUCTION

Silica is extensively used as support for polyolefin catalysts.[1–4] Silica hydrogel is usually made by neutralizing sodium silicate with an acid.[5,6] Silica support physical properties such as surface area, pore volume, and radius of curvature or average pore diameter should be designed and developed during support preparation. Numerous experimental and theoretical works have been done to understand the influence of support on polyolefin catalyst properties.[7–13] To show how the new results achieved in this article can facilitate the understanding of the influence of support porosity on catalyst performance, some important variables discussed on published papers were selected as described below.

- Catalyst fragmentation occurs eventually in the early stage of polymerization. The ability of the support for fragmentation is an essential requirement for an applicable catalyst system which fragments down to the nanometer scale and guarantees a high activity and productivity of catalyst. Fragmentation depends mainly on two factors: hydraulic pressure generated by the formed polymer inside the catalyst pores and the rigidity of the support material.[14–18]
- Polymer/catalyst particle morphology is affected greatly by catalyst fragmentation.[19–21] Homogeneity in fragmentation is a prerequisite to obtain some properties like transparent products since small enough fragments do not scatter light. The mechanism of catalyst/polymer particles evolution has been studied by several research groups and different models have been presented e.g., tension model, meso scale model, and visco-elastic model.[22–24]
- Catalyst particle fragmentation is believed to be responsible for determining of the polymerization rate step and time profile of catalyst activity.[11,25] Mass and energy balances are often governed by the catalyst activity profile during its residence time in reactor.[26]
- The porosity of support plays a major role in determining the molecular weight (MW) and molecular weight distribution (MWD).[9,10,27]

Despite of extensive investigations on the effect of porosity including pore volume, pore surface area, and pore volume distribution on catalyst performance,

Correspondence to: H. Arabi (H. Arabi@ippi.ac.ir).

TABLE I
Characteristics of Supports Corresponding Catalysts Polymerization Conditions and Polymer Products

Support (SiO_2)			Catalyst		Polymerization conditions				Characterization		
Num	APV[a] ($cm^3\ g^{-1}_{SiO2}$)	APD[b] (Å)	SA[c] ($m^2\ g^{-1}$)	Run	CAT (mg)	CoCAT (mmol)	P_{C2} (bar)	1-Butene (mmol L^{-1})	Yield (g)	T_m (°C)	Crys%
SS1	1.15	150	306	CS1R1	30	3	5	0.0	125	135.7	60.6
				CS1R2	40	3	4	9.5	103	131.5	51
				CS1R3	40	3	3	4.5	70	134	stepwise
SS2	0.75	60	490	CS2R1	40	3	5	0.0	106	135.9	56.8
				CS2R2	48	3	7	5.2	112	127.1	57
				CS2R3	32	3	5	9.5	85	130.6	stepwise
SS3	1.63	235	277	CS3R1	33	3	4	0.0	104	135.3	58.1
				CS3R2	33	3	4	4.6	75	127.8	41.4
				CS3R3	33	3	4	9.5	64	126.5	stepwise
SS4	1.75	295	245	CS4R1	35	3	3	0.0	85	135.6	50.8
				CS4R2	35	3	3	5.2	110	126.6	41.2
				CS4R3	33	3	3	9.5	45	127.1	stepwise
SS5	2.2	330	270	CS5R1	33	3	3	0.0	67	135.4	60.3
				CS5R2	42	3	3	4	105	128	50.8
				CS5R3	33	3	3	8	42	132	stepwise
SS6	1.5	198	303	CS6R1	45	3	5	0	111	135.7	57.7
				CS6R2	45	3	4	5	58	125.7	45.8
				CS6R3	45	3	5	10	40	130	stepwise

All supports have particle size distribution 32–64 μm analyzed by sieve.
[a] Average pore volume was obtained from pore size distribution plot, and by BJH method.
[b] Average pore diameter was obtained from Eq. (1).
[c] Average surface area obtained from 5 point BET method.

the relationship between these parameters and catalyst performances such as activity profile, comonomer incorporation, as well as polymer properties are not clear and it requires further investigations. In current work a series of silica support with different porosity were prepared and used in polymerization of ethylene/butene-1 with the aim of finding out clear relations between mentioned factors and applying them to design new tailoring catalyst and products.

EXPERIMENTAL

Materials

Polymerization grade of ethylene, butene-1 (99.5%) was obtained from Bandar Imam Petrochemical (BIP). Hydrogen and nitrogen gases (99.99%) were supplied by Roham Gas, Tehran, Iran. All gases were further purified with preactivated columns packed with molecular sieves that adsorb humidity, CO_2, and sulfur compounds. *N*-Heptane was purifed by refluxing over CaH_2 and distilled before use. Silica gels (grades 644, 633), dibutylmagnesium, tetraethoxy orthosilicate (TEOS), and silane tetrachloride ($SiCl_4$) were purchased from Aldrich. Sodium silicate from Gazvin Silicat, $TiCl_4$ from Merck, and triethylaluminum ($Al(Et)_3$) from Akzo Corp were prepared.

Support preparation

Silica supports (SS) with different physical properties were synthesized by the sol–gel method as follows.[28]

In a typical silica gel preparation method, about 200 g of 31 wt % solution of $(SiO_2)x(Na_2O)y$ in water was poured into a 1-L glass reactor equipped with the stirrer and temperature controller. Then it was diluted by additional 200 cm^3 deionized water and cooled down to below 0°C. Various pH were selected by addition of H_2SO_4 (10 wt %). The temperature of prepared silica gel was increased to 90–100°C and it was allowed to age for different times. After aging, it was washed several times with deionized water to remove the residual Na^+ content. To reduce surface tension and in turn shrinkage effect before drying, the water content of silica gel was replaced by a solvent with lower surface tension like acetone. Silica support samples were assigned SS1-SS6 as shown in Table I.

Catalyst preparation

Catalyst preparation procedure has been described in detail previously.[29] Catalyst samples were assigned as CS1-CS6 based on parent SS1-SS6 silica supports and presented in Table I.

Polymerization

The polymerization reactions were carried out in a 1 dm^3 reactor equipped with a mechanical stirrer. The reactor was filled with hexane (0.5 dm^3), required amounts of $AlEt_3$, and the catalyst precursors (see CS1 to CS6 of in Table I). Then the reactor was pressurized by required amount of butene-1 and ethylene, respectively. Total pressure was kept constant

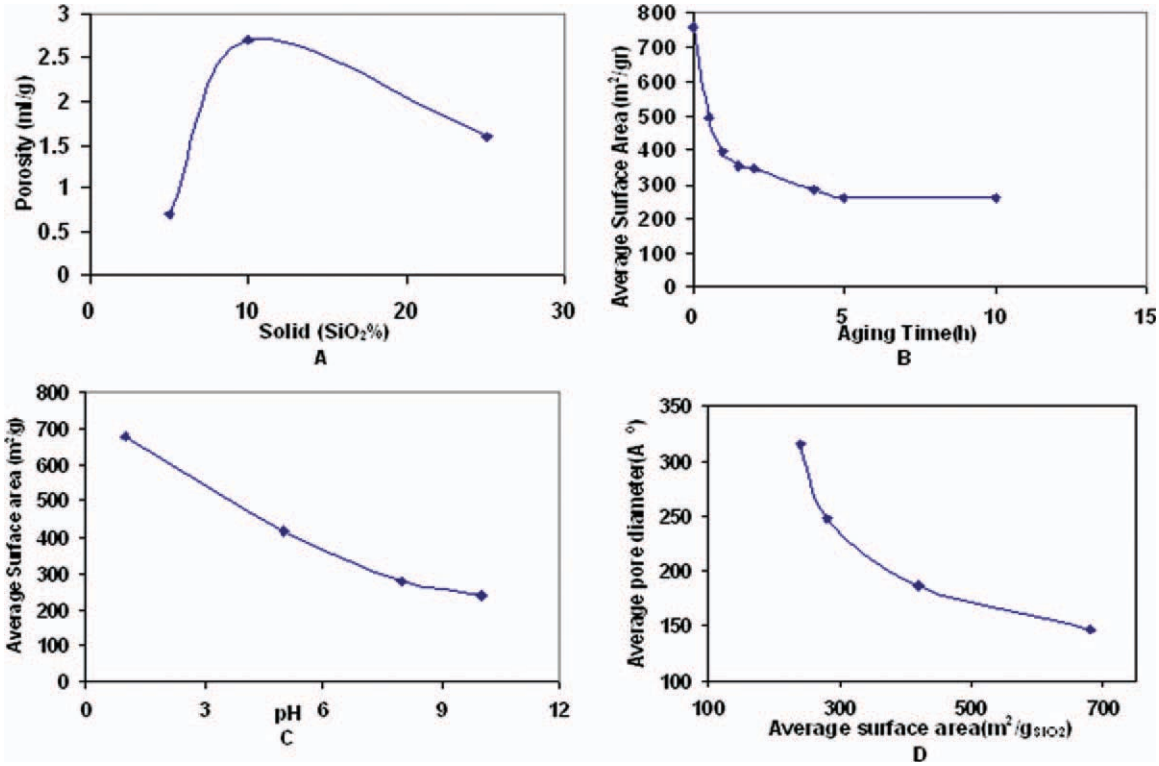

Figure 1 The effects of operation parameters on SiO_2 properties: (A) Effect of SiO_2 final solid content, (B) aging time of hydrogel, (C) pH of aging step, and (D) the relationship between average pore diameter and average surface area obtained from BJH and BET methods, respectively. [Color figure can be viewed in the online issue, which is available at wileyonlinelibrary.com.]

by ethylene feed (activity profile) during polymerization. Table I shows the polymerization conditions for different runs based on various supports and the resulting catalysts.

Characterization

Silica supports

Silica gel samples were degassed at 200°C for 2 h. Adsorption-desorption nitrogen isotherms were measured at −196°C using Quantachrome NOVA. Specific surface area were determined by the Brunauer-Emmett-Teller (BET) Equation (P/P_0 = 0.05–0.95). The mesopore size and distribution were calculated by the Barrett-Joyner-Halenda (BJH method) using the Halsey standards methods, desorption branch was used.[30] The average pore diameter (APD) was calculated as Eq. (1)

$$\mathrm{APD} = 4^{*}\mathrm{APV}/S \quad (1)$$

where:

APV = Average pore volume obtained from BJH method

S = Average surface area from BET method

The pore surface area distribution was obtained by BJH method data and by using Novawin software.

Polymers

A stepwise annealing procedure was conducted to analyze the chemical composition distribution (CCD) of ethylene/butene-1 copolymers.[31] The temperature was increased up to 160°C at a rate of 10°C min^{-1} and maintained for 10 min for complete melting. The heating-annealing-cooling cycle was repeated at a temperature interval of 5°C from 135 to 25°C and annealing for 50 min for the samples and was finally cooled to 30°C at a rate of 10°C min^{-1}. The chemical composition distribution of ethylene/butene-1 copolymer was determined using a DSC with a heating rate of 10°C min^{-1}. The lamella thicknesses of the fractionated ethylene/butene-1 copolymer were determined using the Thomson-Gibbs Equation.[32]

RESULTS AND DISCUSSION

Porosity specifications

As mentioned, support plays as important and critical parameters in activity profile and fragmentation of catalyst. Investigation was carried out to specify the key physical parameter of support structures on catalyst performance. In Figure 1 the effects of some important operation parameters such as pH, temperature of aging step, and final solid content of

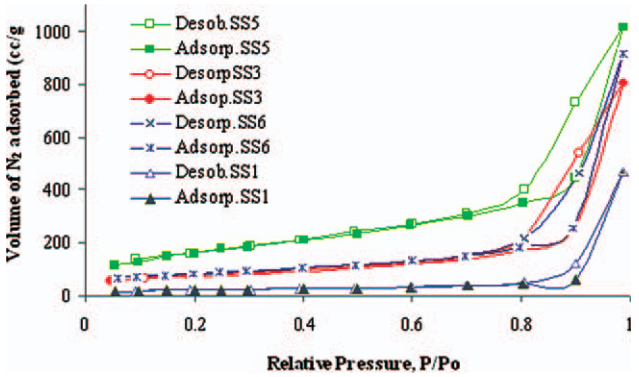

Figure 2 Adsorption–desorption isotherm curves. [Color figure can be viewed in the online issue, which is available at wileyonlinelibrary.com.]

hydrogel on physical properties of supports and variation of average pore diameter as a function of surface area has been illustrated. The Curve 1A shows that for achieving high porosity silica support it is better to operate at about 10 wt % concentration of final solid content of hydrogel. The Curves of 1B, 1C, and 1D demonstrate the aging time of 2 h and pH of 6–8 are suitable to obtain good average surface area (300 m^2 g^{-1}) and PD (250 Å) as favorable specifications.

In Figure 2 the isotherm curves of SS1 to SS6 supports are shown. For adsorption branches with increase in P/P_0 to about 0.8, no considerable variation was observed in pore volume. Beyond this value there is a steep rise in pore volume. Desorption branch also contains a steep region associated with a closure of the hysteresis loop. According to IUPAC porous material classification, silica supports show typical curve of nonrigid aggregates of submicron particles giving rise to curvature-shape pores.[33]

A closer look at Figure 2 isotherms shows similar shape but different APV, in which support SS5 and support SS1 have highest and lowest pore volume, respectively.

Figure 3 shows the variation of pore volume, DV (log d), versus pore diameter (d). These profiles are

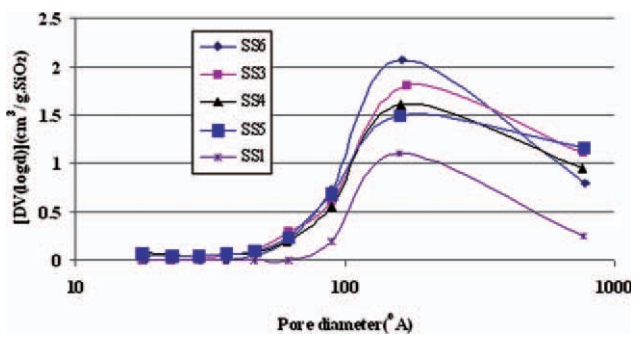

Figure 3 The variation of pore volume of various silica supports. [Color figure can be viewed in the online issue, which is available at wileyonlinelibrary.com.]

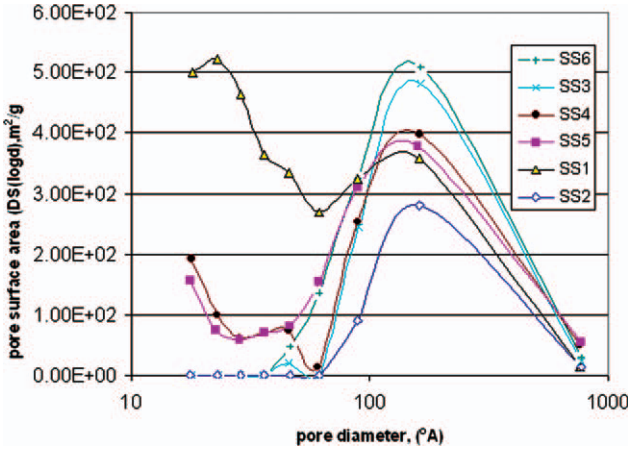

Figure 4 Variation of pore surface area versus pore diameter. [Color figure can be viewed in the online issue, which is available at wileyonlinelibrary.com.]

arising from desorption branch data of isotherm which had been calculated based on BJH method.

It can be concluded from Figure 3 that pore volume which correspond to pores with diameters below 90 Å is very small. Also negligible and all profiles have the same maximum peak point at about 200 Å. On the hand, SS5 and SS3 supports give higher pore volume at upper limit of pore diameter distribution. Calculations of total pore volumes show that SS5 gives higher pore volume and bigger pore average diameter, while SS4 to SS1 are placed successively in next steps.

In Figure 4 the variation of PSAD as a function of PD are shown.

With regard to variations of pore surface area two distinguishable regions below and above PD of 90 Å can be observed. For most of supports moving to lower PD of 90 Å, pore surface area increased mainly for SS1 and with a lesser degree for SS4 and SS5. Supports SS2 and SS6 show unimodal PSAD. Beyond PD of 90 Å a Gaussian distribution can be observed.

The effect of porosity on copolymerization activity

Figure 5 shows the activity profiles of ethylene polymerization for CS1-CS6 with different concentration of butene-1 ($R1 = 0$, $R2 = 0.3$ mmol L^{-1} and $R3 = 10$ mmol L^{-1}). Figure 5(B,E) illustrate the activity profile variations for CS2 and CS5 catalysts. These catalysts have 0.75 cm^3 g^{-1}_{SiO2} and 2.2 cm^3 g^{-1}_{SiO2}, lowest and highest porosity, respectively. In catalyst CS2 in the presence of comonomer the activity of polymerization sharply raised and then drastically fell down while in absence of comonomer activity gradually increases and remains stable and then steadily decreases. Figure 5(F) shows that CS5 catalyst has highest response to the presence of comonomer and activity of polymerization increased by two to three times.

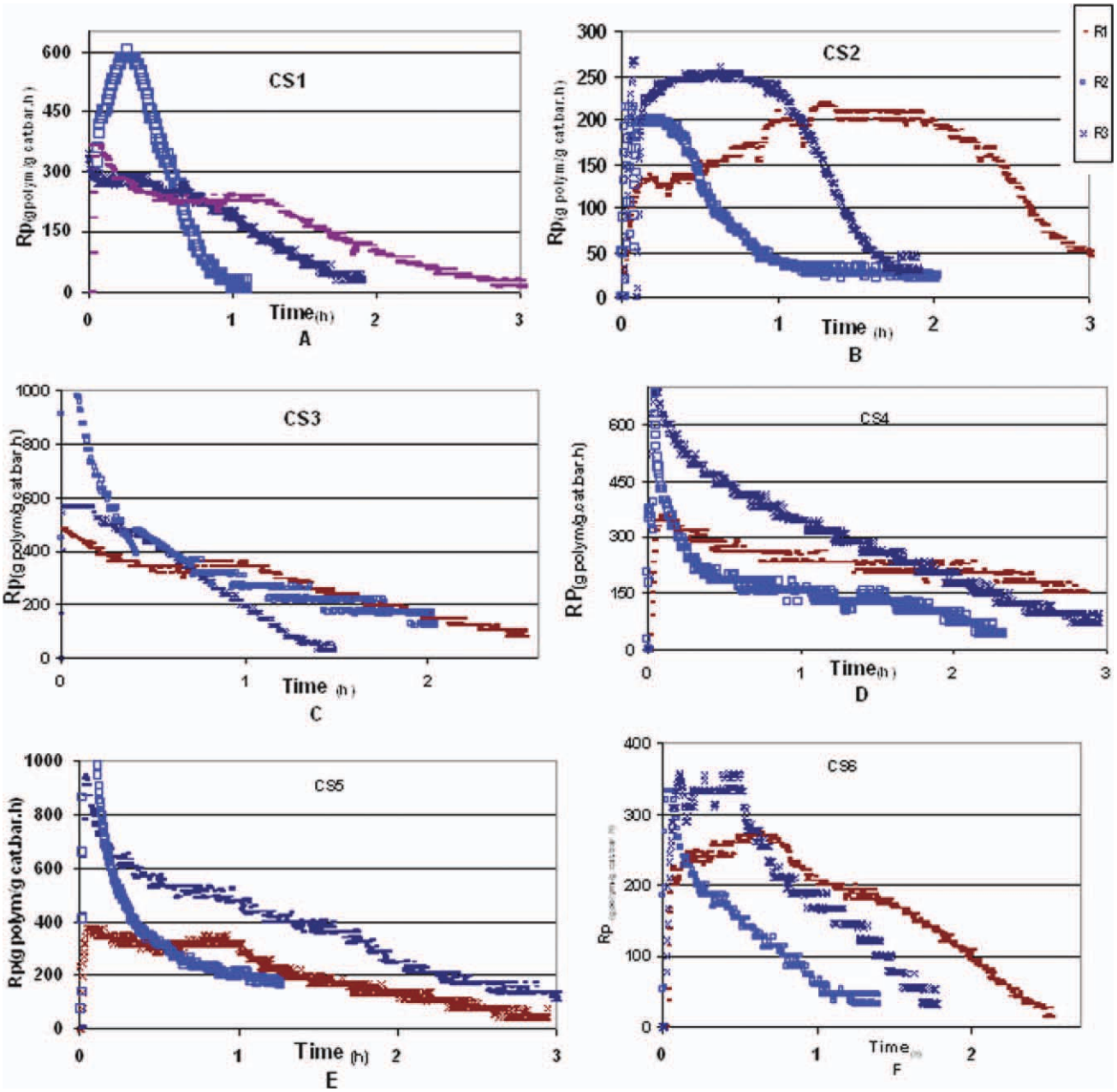

Figure 5 Activity profiles of ethylene/butene-1 copolymerization by catalysts CS1 to CS6 according to Table I condition. [Color figure can be viewed in the online issue, which is available at wileyonlinelibrary.com.]

For catalysts of CS1, CS3, CS4, and CS5, secondary peak at activity profiles can be observed. This behavior can be attributed to the increased surface area in two regions as shown in Figure 4.

Runs R3 in Figure 5 of CS1 and CS5 catalyst show a unexpected decrease in activity compared to other runs. The silica supports of this catalyst have higher pore volume among all others and when comonomer concentration exceeds certain value this behavior appears. This led to formation of continuous gel-like product which limits monomere and cocatalyst transfer to active sites, causing a sudden fall in activity.

In summary, it can be suggested that in the early stages of polymerization because of comonomer incorporation, the crystalline phase is reduced and it decreases the effect of probable mass transfer limitation from the bulk to the inner active sites. This results in sharp acceleration in initial activity profiles.

Besides, the amount of comonomer has an opposite effect on activity profile and productivity so that increasing comonomer concentration to certain values ensures increasing of activity, while extra concentration has inverse effect on productivity.

It is generally confirmed that, activity profiles are mainly affected by two factors, intrinsic activity of catalyst site[2–4] and fragmentation phenomena.[34–38] For catalyst with small particle size (below 10 μm),

intrinsic activity is dominant factor and it determines the shape of activity profile, but with larger particle size, (60–100 μm) e.g., gas phase catalyst, there are complex interaction between fragmentation and intrinsic site-activity which governs final activity profile. When polymer is formed in the catalyst particle, the molecular chains grow and break the agglomerated silica support particles into small particles.

Supports provide a distribution of porosity or pores volume in whole catalyst particle, which need a spectrum of stress to precede fragmentation during polymerization. Comonomer can influence the fragmentation behavior in two contrary ways,[38,39] first by increasing catalyst activity which in turn creates higher polymer and stress and therefore accelerate catalyst fragmentation and second in high concentration, by lowering the stress relaxation time via increasing polymer mobility. It was being noticed that the effect of increasing active-site reactivity is more pronounced for early times of polymerization while the effect of polymer mobility increasing manifests in the late stage of polymerization. In this point, fragmentation is advanced to very small pore diameters and greater stress is needed to keep on fragmentation. Therefore, significant decrease in activity profile can be observed.

To quantify the effect of supports specification on polymerization behavior a simple model on the basis of the following assumption was proposed.[5,10]

1. Silica gel catalyst particles are consisting of agglomerated subparticles which form different pore diameter distribution and polymerization initiation occurred in priority in larger pore diameter and extends to smaller pore diameter.
2. Fragmentation phenomena start from larger pore volume with weaker structure strength and extend to lower pore volume.
3. The hydraulic stress of fragmentation is provided by agglomerating of produced polymer, in pores of catalyst particle and it depends on polymerization condition, support strength, and polymer properties (stress relaxation).

The catalyst active site which can be available conform to kinetics mechanism had been presented by Kissin and coworkers[2–4] and in this study Eq. (2) derived based on this mechanism.

$$R_p^j = Q^j \frac{\exp(-k_a t) - \exp(-k_d t)}{\frac{1-\exp(-k_a t_{\text{reaction}})}{k_a} - \frac{1-\exp(-k_d t_{\text{reaction}})}{k_d}} \tag{2}$$

By extending Kissin kinetics mechanism and adding up fragmentation phenomena in simplified way, the new model for calculation of kinetic constants and discerning fragmentation times was developed [Eq. (3)]. By fitting experimental data with new

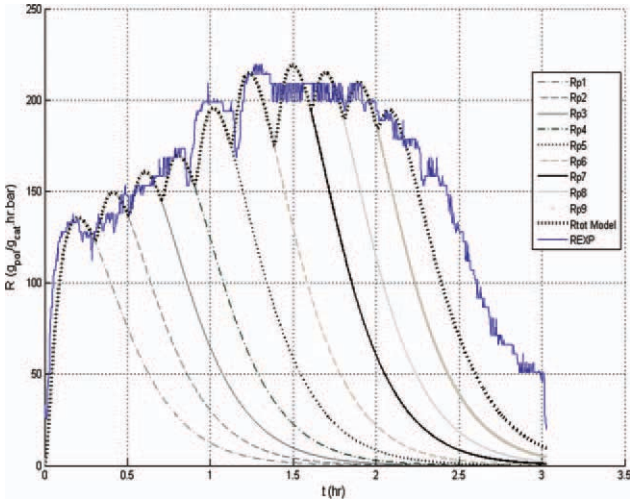

Figure 6 Curve fitting of activity profile of CS2R1 run of polymerization according to Eq. (4) by 10 of individual fragments. [Color figure can be viewed in the online issue, which is available at wileyonlinelibrary.com.]

derived Eq. (4), kinetics constants and fragmentation parameters can be calculated.

$$R_p^j = Q^j \frac{\exp(-k_a(t - t_f j)) - \exp(-k_d(t - t_f j)}{\frac{1-\exp(-k_a(\Delta tfj))}{k_a} - \frac{1-\exp(-k_d(\Delta tfj)}{k_d}} u(t - tfj) \tag{3}$$

$$R_p = \sum_{j=1}^{n} R_p^j \tag{4}$$

$$\text{PI} = \sum_{i=1}^{n} [R_p^{\text{EXP}}(i) - R_p^{\text{Theor}}(i)]^2 \tag{5}$$

R_p Overall activity profile
R_p^j Activity rate profile of jth fragments
Q^j Required yield to create enough stress for fragmentation
tfj Required time to occur jth fragments
k_d Catalyst deactivation constant
k_a Catalyst activation constant
t Polymerization time
R_p^{EXP} Experimental catalyst activity profile
PI Optimization function
Δtfj Difference of two sequential fragmentation times.

By using GaTool Optimization subprogram of MATLAB software ver.7 through minimizing Eq. (5), experimental data's of activity profiles (CS1R1 to CS6R3 polymerization runs) were fitted to Eq. (4), and catalysts activity parameters including times of fragmentations (tfj), tfj is the time in which the catalyst particles undergoes jth fragmentation, required fragmentation stress as a measure of yield (Q^j) and kinetic constants (k_a and k_d) were calculated. In Figures 6 and 7 typical curves fitting by supposing

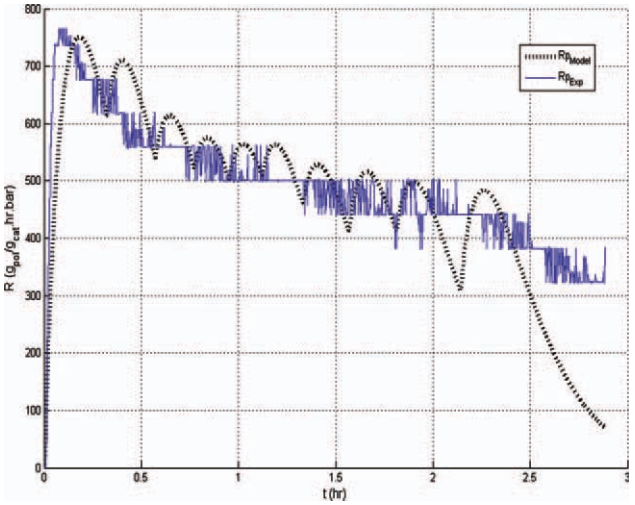

Figure 7 Curve fitting of activity profile of CS4R1 run according to Eq. (4) with 10 of individual fragments. [Color figure can be viewed in the online issue, which is available at wileyonlinelibrary.com.]

10 fragments for CS1R1 and CS5R1 are illustrated. For simplifying calculations Δtfj were taken equal. Resulted activity constants are presented in Table II.

Obtained results demonstrate suggested model has an appropriate ability in fitting of experimental curves and deriving kinetic parameters.

The results showed that fragmentation times (*tfj*) for catalysts with high pore volume are shorter than those with small pore and higher yield required *Qj* to accumulate the necessary stress for fragmentation of high pore volume catalyst. The values of *Qj* are bigger in high pore volume catalyst as seen in Table II. However, the required stress is lower due to lower mechanical strength. For catalyst with larger pore diameter, k_a and k_d play greater role in activity profile shape while for catalyst with low and small pore diameter *tfj* and *Qj* are dominant.

The effect of porosity on comonomer incorporation

To investigate the effect of support porosity on comonomer incorporation and copolymer properties, thermal behavior of produced copolymers were studied. Stepwise DSC was used to probe composition distributions by attempting to fractionate copolymers on the basis of the segment length between branches. Figure 8 shows the temperature program for stepwise heating-annealing-cooling cycle as described earlier and in Figure 9 the stepwise DSC of copolymers prepared by catalysts listed in Table I are presented. Melting temperatures of these copolymers were considerably diminished with increasing average pore diameter which means that more comonomer incorporates in chains.

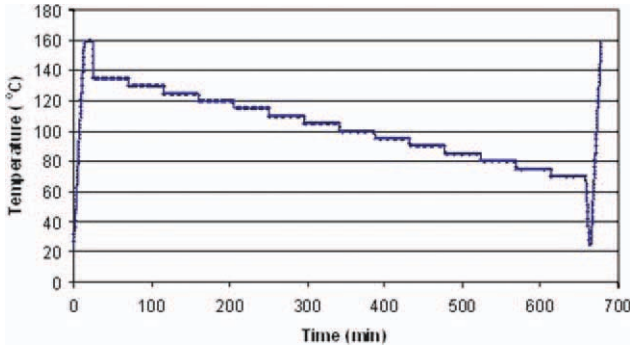

Figure 8 Stepwise DSC thermal program. [Color figure can be viewed in the online issue, which is available at wileyonlinelibrary.com.]

Stepwise DSC data of Figure 9 were analyzed by using Peakfit software and deconvoluted based on Lorentz distribution function. Figure 10 shows the typical deconvolution of CS2 catalyst. It can be supposed that each peak corresponds to a lamella with certain thickness and its surface area indicates the percentage of that crystallite phase. Gibbs-Thomson and Hosoda Equations [eqs. (6) and (7)], respectively, are used to study the relationship between thermodynamic driving force for crystallization and the branching content of a chain.

Gibbs Thomson Equation

$$T_m = T_m^o(1 - 2\delta/\Delta H_u L_C) \quad (6)$$

where T_m is melting point and L_C is the thickness of the lamella. T_m^o is the equilibrium melting point of an infinite polyethylene crystal ($T_m^o = 418.7$ K). δ is the surface energy per unit area of the basal face (87×10^{-3} J m^{-2}) and is associated with the energy of chain folding during crystallization; and ΔH_u is the enthalpy of fusion per unit volume (290×10^6) J m^{-3}.[40]

Hosoda Equation

$$T(^\circ C) = -1.6 \times SCB + 136 \quad (7)$$

SCB: Short Chain Braching

T: Melting point

TABLE II
Activity Constants of CS1R1 and CS5R1 Runs Based on Eq. (4)

Catalyst run	Q_p^1	Q_p^2	Q_p^3	Q_p^4	Q_p^5	Q_p^5	Q_p^6	Q_p^7	Q_p^8	Q_p^9	Δtfj	k_a	k_d
CS1R1	240	85	85	90	130	150	150	100	100	100	0.2	2	2.3
CS5R1	1600	536	412	311	300	315	380	450	470	450	0.2	5.5	15

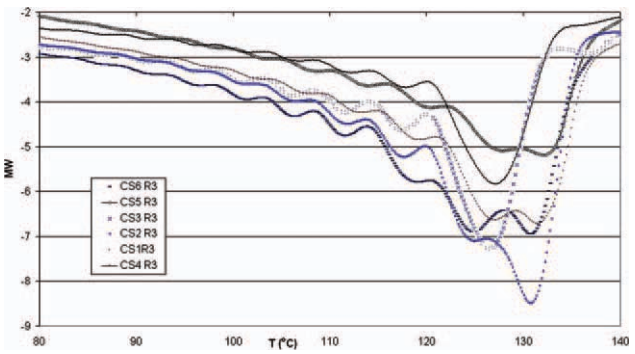

Figure 9 Stepwise DSC thermogram of copolymer of catalysts assigned in Table I. [Color figure can be viewed in the online issue, which is available at wileyonlinelibrary.com.]

Polymer chains with more short chain branches crystallize at lower temperatures, forming thinner lamellae and less perfect crystallites. In Figure 11 the weight percentage of different crystallites versus their comonomer distribution content for samples SC1R3 to SC6R3 are illustrated.

From Figure 11 it can be concluded that catalyst with higher pore volume gives copolymer with higher amount of comonomer and interestingly, the distribution of comonomer is more homogenous.

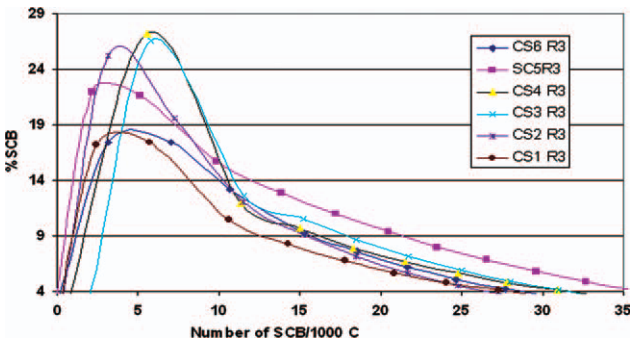

Figure 11 Short chain branching (SCB) distribution in different copolymers. [Color figure can be viewed in the online issue, which is available at wileyonlinelibrary.com.]

CONCLUSIONS

A series of different SiO_2 supports were prepared and after characterizing their physical properties used in synthesis of corresponding catalysts. To investigate the effects of support properties e.g., APV, PD, and PSAD on activity profile, and also comonomer incorporation and polymer properties, polymerization of ethylene/butene-1 was carried out by synthesized catalysts. Conventional Z-N catalyst mechanism was modified by introducing fragmentation term and a

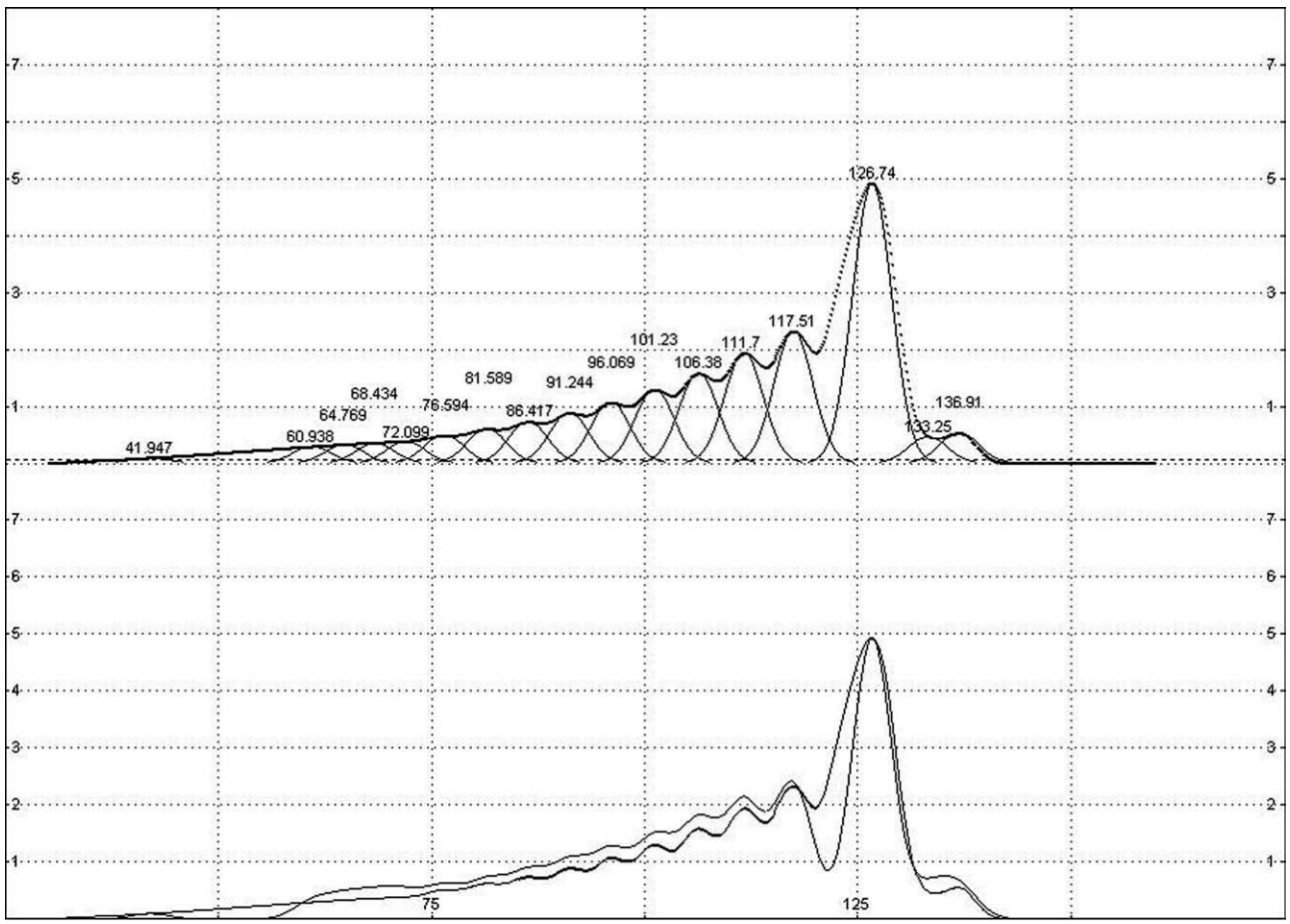

Figure 10 Decovoluted stepwise DSC themograms based on Lorentzian function.

new kinetic equation for quantitative studying of support specification was developed. Stepwise DSC was used to probe comonomer distributions. Comparing experimental activity profiles and comonomer distributions showed that activity and shape of activity profile are controlled significantly by average pore volume and pores surface area distribution, respectively. Enhancing pore volume from 0.75 to 2.2 cm^3 g_{cat}^{-1} increased initial activity more than two times and catalysts with higher pore diameters give more comonomer incorporation and more homogenous products.

References

1. Garoff, T.; Vaananen, M.; Root, A.; Stalhammar, M.; Pesonen, K. Eur Polym J 2007, 43, 5055.
2. Nowlin, T. E.; Kissin, Y. V.; Wagner, K. P. J Polym Sci Part A Polym Chem 1988, 26, 755.
3. Kissin, Y. V.; Mirabella, F. M.; Meverden, C. C. J Polym Sci Part A Polym Chem 2005, 43, 4351.
4. Karakalos, S.; Siokou, A.; Ladas, S. Appl Surf Sci 2009, 255, 8941.
5. Bergna, H. E. In The Colloid Chemistry of Silica, ACS Advances in Chemistry Series 234; Urban, M. W., Grauer, C. D., Eds.; ACS: Washington DC, 1994; Chapter 1, p 1.
6. Korach, L.; Czaja, K.; Kovaleva, N. Y. Eur Polym J 2008, 44, 889.
7. Kakugo, M.; Sadatoshi, H.; Sakai, J.; Yokoyama, M. Macromolecules 1989, 22, 3172.
8. Estenos, D. A.; Chiovetta, M. G. J Appl Polym Sci 2001, 81, 285.
9. McDaniel, M. P. J Catal 2009, 261, 34.
10. Bartke, M.; Severn, J. R.; Chadwick, J. C. Tailor-Made Polymers Via Immobilization of Alpha-Olefin Polymerization Catalyst; Wiley-VCH Verlag GmbH & co KGaA: Weinheim, 2008; p 79.
11. Hammawa, H.; Wanke, S. E. J Appl Polym Sci 2007, 104, 514.
12. Hammawa, H.; Wanke, S. E. Polym Int 2006, 55, 426.
13. McKenna, T. F.; Soares, J. B. P. Chem Eng Sci 2001, 56, 3931.
14. Ferrero, M. A.; Chiovetta, M. G. Polym Eng Sci 1991, 31, 904.
15. Ronkko, H. L.; Korpelaa, T.; Knuuttila, H.; Pakkanen, T. T.; Denifl, P.; Leinonen, T.; Kemellc, M.; Leskela, M. J Mol Catal Chem 2009, 309, 40.
16. Abboud, M.; Denifl, P.; Reichert, K. H. Macromol Mater Eng 2005, 290, 558.
17. Horackova, B.; Grof, Z.; Kosek, J. Chem Eng Sci 2007, 62, 5264.
18. Silva, F. M.; Broyer, J. P.; Novat, C.; Lima, E. L.; Pinto, J. C.; McKenna, T. F. Macromol Rapid Commun 2005, 26, 1846.
19. Schulz, R. C. Macromol Chem Phys 2005, 206, 2027.
20. Abboud, M.; Denifl, P.; Reichertl, K. H. J Appl Polym Sci 2005, 98, 2191.
21. Naik, S. D.; Ray, W. H. J Appl Polym Sci 2001, 79, 2565.
22. Zheng, X.; Loos, J. Macromol Symp 2006, 236, 249.
23. Grof, Z.; Kosek, J.; Marek, M. AIChE J 2003, 49, 1002.
24. Agarwal, U. S.; Lemstra, P. J Chem Eng Sci 2001, 156, 4007.
25. Nakatani, H.; Matsuoka, H.; Suzuki, S.; Taniike, T.; Boping, L.; Terano, M. Macromol Symp 2007, 257, 112.
26. Wells, G. J.; Ray, W. H. AIChE J 2001, 47, 401.
27. Zheng, X.; Pimplapure, M. S.; Weickert, G.; Loos, J. Macromol Rapid Commun 2006, 27, 15.
28. Hyde, J. R. Microspheroidal Silica Gel, Grace, W R & Co, CA patent 8,11,107, 1969.
29. Vakili, M.; Arabi, H.; Salehi Mobarake, M.; Ghafelebashi, M. J Appl Polym Sci 2010, 118, 2216.
30. Lowell, S.; Shields, J. E.; Martin, A.; Matthias, T. Characterization of Porous Solids and Powders: Surface Area, Pore Size, and Density; Springer, Dordrecht, 2006; p 20.
31. Zhang, X.; Lynch, D. T.; Wanke, S. E. Polymer 2001, 42, 3067.
32. Zhou, H.; Wilkes, G. L. Polymer 1997, 38, 5735.
33. Starck, P. Polym Int 1996, 40, 111.
34. Fink, G.; Tesche, B.; Korber, F.; Knoke, S. Macromol Symp 2001, 173, 77.
35. Conner, W. C.; Webb, S. W.; Spenne, P.; Jones, K. W. Macromolecule 1990, 23, 4742.
36. Grof, Z.; Kosek, J.; Marek, M. Ind Eng Chem Res 2005, 44, 2389.
37. Kakugo, M.; Sadatoshi, H.; Yokoyama, M.; Kojima, K. Macromolecules 1989, 22, 547.
38. Grieken, R.; Carrero, A.; Suarez, I.; Pare, B. Macromol Symp 2007, 259, 243.
39. Smit, M.; Zheng, X.; Bru, R.; Loos, J.; Chadwick, J. C.; Koning, C. E. J Polym Sci Part A Polym Chem 2006, 44, 2883.
40. Hosoda, S. Polym J 1988, 20, 383.